

## Article

# Formation of Humic-Like Substances during the Technological Process of Lignohumate<sup>®</sup> Synthesis as a Function of Time

Olga Yakimenko<sup>1,\*</sup>, Andrey Stepanov<sup>1</sup>, Svetlana Patsaeva<sup>2</sup>, Daria Khundzhua<sup>2</sup>, Olesya Osipova<sup>3</sup> and Oleg Gladkov<sup>3</sup>

<sup>1</sup> Department of Soil Science, Moscow State University, Leninskie Gory 1-12, 119992 Moscow, Russia; stepan.1963@mail.ru

<sup>2</sup> Department of Physics, Moscow State University, Leninskie Gory 1-2, 119992 Moscow, Russia; patsaeva@physics.msu.ru (S.P.); dasha.ok@list.ru (D.K.)

<sup>3</sup> LTD RET, Malookhtinsky pr. 61 A, Office 210, 195112 St-Petersburg, Russia; o.gladkov48@mail.ru (O.O.); gladkov@humate.spb.ru (O.G.)

\* Correspondence: iakim@soil.msu.ru

**Abstract:** The composition, structure, and biological activity of humic-like substances (HLS) synthesized in the process of lignosulfonate conversion for the production of the humic product Lignohumate<sup>®</sup> (LH) were examined. It is shown that during the hydrolytic-oxidative process, the transformation of raw material and accumulation of HLS occur. Data on the chemical (elemental content, functional groups, FTIR) and spectral (absorbance and fluorescence) parameters and biological activity (in phytotest) combined with PCA show that the LH samples can be divided into three groups, depending on the duration of synthesis: initial raw material (0-time sample); “young” HLS (15–30 min), and “mature” HLS in 45–120 min of treatment. During the first 30 min, reactions similar to the ones that occur during lignin humification in nature take place: depolymerization, oxidative carboxylation, and further polycondensation with the formation and accumulation of HLS. After 45–60 min, the share of HLS reaches a maximum, and its composition stabilizes. Biological activity reaches a maximum after 45–60 min of treatment, and at that stage, the further synthesis process can be stopped. Further processing (up to 2 h and more) does not provide any added value to the humic product.

**Keywords:** Lignohumate; humic-like substances; absorbance; fluorescence; FTIR; bioassay; PCA



**Citation:** Yakimenko, O.; Stepanov, A.; Patsaeva, S.; Khundzhua, D.; Osipova, O.; Gladkov, O. Formation of Humic-Like Substances during the Technological Process of Lignohumate<sup>®</sup> Synthesis as a Function of Time. *Separations* **2021**, *8*, 96. <https://doi.org/10.3390/separations8070096>

Academic Editor: Denis Pankratov

Received: 30 May 2021

Accepted: 1 July 2021

Published: 3 July 2021

**Publisher's Note:** MDPI stays neutral with regard to jurisdictional claims in published maps and institutional affiliations.



**Copyright:** © 2021 by the authors. Licensee MDPI, Basel, Switzerland. This article is an open access article distributed under the terms and conditions of the Creative Commons Attribution (CC BY) license (<https://creativecommons.org/licenses/by/4.0/>).

## 1. Introduction

Humic-based amendments (humic product, HP) are increasingly used in agriculture [1–6] and are being currently considered as a major category of biostimulants [7,8]. HPs are manufactured by industrial companies from various humic resources (mostly lignite, peat, and composts), as well as lignocellulose wastes [9–12]. The chemical composition and effectiveness of HPs as plant growth stimulators vary depending on the organic matter source, extraction processes (KOH extraction for lignite, cavitation for peat, wood bisulfite extraction for lignosulfonates, etc.), and modification technologies used to obtain the products [13–15]. Therefore, the chemical characterization of marketed HPs combined with the testing of their efficiency as biostimulants is a relevant, comprehensive task.

Lignosulfonate (LS), the wood-processing byproduct, is one of the possible source organic materials for HP production. There are contradictory opinions concerning its possible functioning as an HP. Some publications report a positive role of LS in crop growth [16–20], whereas others consider it as a “fake” HP that can serve only as a stabilizer of HP solutions with a minor effect on plant growth [21,22]. However, by all means, LS is a valuable organic raw material, sharing similar properties with humic substances in terms of an aromatic core with carboxylic and phenolic functional groups. The appropriate

technological treatment of LS can result in the production of qualitative HP and contribute to the important environmental task of converting lignin-containing organic wastes [23–25].

The LTD RET Company (St-Petersburg, Russia) has developed and patented an industrial technology for the conversion of technical LS with the following synthesis of a number of humic-like biologically active substances (HLS) [26], which finally compose the commercial humic product Lignohumate<sup>®</sup> (LH). Their technology is based on the thermal hydrolytic–oxidative conversion of technical lignosulfonates (LS) under high pressure. The technical LSs are sulfonated lignins obtained during the sulfite cooking of wood [18,27,28]. Delignification in sulfite pulping involves acidic cleavage of ether bonds, which connect many of the lignin constituents. The primary site for the ether cleavage is a carbon atom attached to the aromatic ring of the propyl side chain [29].

The conversion of technical lignosulfonates to HLS runs under regulated and strictly controlled conditions in continuous oxidative mode. Details of the technological process are provided in Section 2.1. In brief, the initial LS is mixed with potassium hydroxide in the reaction tank, and the obtained alkaline solution is processed under elevated pressure and temperature with a constant supply of air. During the hydrolytic-oxidative process, the transformation of LS and synthesis of HLS occurs. The final product is continuously discharged from the reaction zone to the product tank.

The oxidation of LS by molecular oxygen in alkaline media leads to lignin decomposition and produces phenolic aldehydes, phenolic acids, and carboxylic acids [30,31]. The oxidative cleavage of LS to aromatic aldehydes comprises alkaline hydrolysis and autoxidation steps [32,33]. The alkaline hydrolysis at pH above 11 includes the retro-aldol cleavage of benzyl alcohol-type structures containing  $\gamma$ -carbonyl groups [32,34]. The C $\alpha$ -C $\beta$  oxidative cleavage of the propane chain in the LS structural units, the main reaction pathway leading to the formation of aromatic aldehydes, proceeds under alkaline conditions only (pH > 10). The role of the base consists of the partial desulfonation of LS with the formation of unsaturated C $\alpha$ -C $\beta$  moieties (enol-, stilbene-, and diene-type structures) and ionization of the phenoxyl, thus reducing the energetic barrier in reaction with oxygen [35]. The yield of aromatic aldehydes is affected by temperature (>120 °C) and oxygen partial pressure (>1 bar) [36,37].

In turn, the monomeric phenolic products of LS decomposition in alkaline media are subjected to further condensation via radical coupling [25,32]. Considering the presence of residual carbohydrates and a minor amount of residual amino acids in technical LS, this process can be conventionally regarded as an imitation of the evolutionary process of natural lignin transformation and/or humification, accelerated hundreds of thousands of times. It considers only the chemical (abiotic) factors of transformation of lignin-containing organic matter; therefore, it is free of metabolization, and most of the carbon ends up as HLS or is released as gases.

Thus, depending on the technological regimes used in LH production (alkali content, changes in temperature, pressure, oxidation rate, and time), the composition and properties of the obtained final product can be different. The yield and biological activity of the synthesized HLS can also change with the course of the technological process.

Therefore, the technology is constantly being updated and improved to achieve the highest yield and quality of the humic product. The obtained various LH formulations have been widely tested both in terms of chemical and spectral properties [9,38–41] and as plant growth stimulators and soil conditioners on various crops and environmental conditions [42–44].

In this study, we focused on the possibility of changing the composition of the synthesized humic-like biologically active formulations of LH, based on changing only one of the technological parameters of the process: the duration of synthesis. Attempts to characterize the quality of marketed HP using the structure-property relationships are numerous [14,45–47] but not very successful up to now. Due to the fact that biostimulants improve plant productivity due to emergent properties, but not as a sole consequence of the presence of known compounds [48–50], the total content of humic substances, as well

as their certain molecular features, often do not correlate well with the test-responses in bioassays. Therefore, besides the chemical parameters of LH, we selected plant growth promotion as the basic criteria to evaluate the quality of LH formulations as a function of synthesis time.

The objectives of the study are: (1) to characterize the chemical composition and biological activity of the product (LH) in several samples taken at different times during the technological process; (2) to reveal qualitative differences in LH composition as a function of time and to determine the optimal duration of the process for obtaining a high-quality humic product.

## 2. Materials and Methods

### 2.1. Technological Process and Sampling

LH is produced by liquid-phase oxidation of the mixture of an alkaline agent (potassium hydroxide) with a lignin-containing plant raw material having a total content of dry matter of 12–20% (the by-product of cellulose production by a sulfite process, i.e., concentrated solution of technical LS). The oxidation is conducted in two stages. In the first stage, pre-oxidation is conducted at a temperature of 50–190 °C and a pressure of 0.5–3 MPa associated with the simultaneous treatment with an oxygen-containing gas until a pH of 10.5–12 is reached. The second stage, i.e., oxidation, is performed under similar conditions at a temperature of 170–200 °C until a pH of 8.5–10 is reached [26].

Initial LS in an amount of 100 kg is diluted in 250 L of water and mixed with 12 kg (30% of the mass of organic substances) of KOH diluted in 50 L of water. The mixture is heated in a heat exchanger to a temperature of 180 °C and charged by a dosing pump, through the heat exchanger, to a pre-oxidation reactor through which air is bubbled under a pressure of 2.0 MPa, at a specific flow rate of up to 20–30 nm<sup>3</sup> m<sup>-3</sup>. On reaching a pH of 11, the mass is fed to an oxidation reactor where a temperature of 180 °C is maintained, through which air bubbling is provided at a specific flow rate of 40–50 nm<sup>3</sup> m<sup>-3</sup>, and a pressure of 2.5 MPa is maintained. After a pH of 9.6 is reached, the mass is supplied to a heat exchanger, where it is cooled down to 70°C and then discharged to the final product tank through adjustable shut-off valves.

Samples were taken during the industrial process of LH manufacturing on the LTD RET facility. For the study, we used samples of the initial raw material (LS, 0 min) and samples of LH, taken from the heated working mixture at certain time intervals from the start of the oxidation process: at 15, 30, 45, 60, and 120 min and after a forced two-hour exposure without oxygen supply (conservation; >120 min).

### 2.2. Chemical Analyses

Liquid LH samples were dried at 105°C in a vacuum dryer and analyzed for dry matter (DM) content. Organic matter (OM) and ash content were determined after the ignition of DM in a muffle furnace at 900°C up to constant weight (at least 8 h).

The CHNS contents of the dried samples were analyzed using a «Carlo Erba» analyzer. The O content was determined by difference. The total acidity of the samples was determined by the Ba (OH)<sub>2</sub> method [51]. The extraction and separation of the humic-like fraction (HLF) was performed using an operational methodology. To obtain solutions uniformed by C content and pH, we used the data on DM and C contents in the samples. We took appropriate aliquots of the liquid samples, brought them to pH 12 by adding 0.1 M NaOH, acidified them to pH 1–2 by adding 10% HCl, and heated them in a boiling water bath (40 min). After settling, the precipitated HLS were separated by centrifugation and dried to constant weight in a vacuum dryer. The content of the acid-soluble fulvic-like fraction (FLF) was calculated by the difference between OM and HLF.

### 2.3. UV-Vis Absorption and Fluorescence

Both absorption and fluorescence spectral measurements were made at room temperature for the liquid samples of LS and LH, diluted 10<sup>4</sup> times, and placed in quartz cuvettes

with a 1 cm optical path length and a 5 mL volume. Absorption spectra were measured with a photometer Solar PB2201 against distilled water.

Fluorescence emission spectra were recorded by a luminescence spectrometer Solar CM 2203 under excitation at 270, 310, and 355 nm. The choice of excitation wavelengths was based on our previous reports on LH fluorescence [52] and the chromatographic fluorescent components of dissolved organic matter in natural water [53]. Fluorescence emission spectra were corrected for the possible “inner-filter” effect using absorbance data.

#### 2.4. FTIR Spectra

Dried LH samples (1 mg) were homogenized in an agate mortar and mixed with oven-dried KBr of analytical quality (300 mg). The pellets were pressed with a hydraulic pellet press CrushIR. The infrared spectra were recorded using the KBr-technique and a FTIR-spectrophotometer Tenzor 27 (Bruker Optics) equipped with a Smart Miracle Si crystal attenuated total reflectance (ATR) accessory and a DTGS KBr detector in the wavenumber range 4000–500  $\text{cm}^{-1}$ . Spectra analyses involving atmospheric suppression, advanced ATR correction, and baseline correction were performed using the Opus 7.0 software.

#### 2.5. Plant Growth Bioassay

The biological activity of the LH samples was evaluated in laboratory phytotests as an increment of oven-dry biomass of shoots and roots of radish *Raphanus sativus* (var. Nota). Radish seeds (50 ps) were placed in a sterile Petri dish on two layers of filter paper, and 7 mL of 0.02% solutions of LH samples were poured. In the control, distilled water was used. Seeds were germinated in a thermostat at 23 °C in the dark. On the 5th day of the exposition, the roots and shoots of seedlings were separated from the empty cotyledons, dried in pre-calibrated weighing cups at 105 °C, and weighted. All bioassays were done in triplicate, an ANOVA was conducted to determine statistical differences; the means were compared by the post hoc Fisher’s least significance test.

#### 2.6. Statistical Analysis

The Principal Component Analysis (PCA) was conducted considering the following variables: pH; DM ( $\text{g L}^{-1}$ ), OM (% DM); HLF (% OM); S (%); atomic ratios; total acidity ( $\text{meq g}^{-1}$ ); absorption of phenolic moieties at 285 nm, normalized by OM content; fluorescence intensity at 315 nm (phenolic fluorescence at excitation wavelength 235 nm) and 400 nm (humic-like fluorescence excited at 235 nm); as well as root biomass.

### 3. Results

#### 3.1. Composition of HLS: Elemental Content and Functional Groups

From the beginning of the oxidation, a permanent transformation of OM and synthesis of the HLS take place. The main chemical parameters are reported in Table 1. The initial raw material had a pH of 5.2, and after mixing with alkali, it rose to 11–12 (working solution, data not shown) and then subsequently gradually decreased to 8–9 during the oxidation process. At the same time, in the course of the oxidation process, a gradual synthesis of HLF occurs: the share of HLF in OM was constantly increasing from 30% after 15 min, up to 75% after 2 h (Table 1).

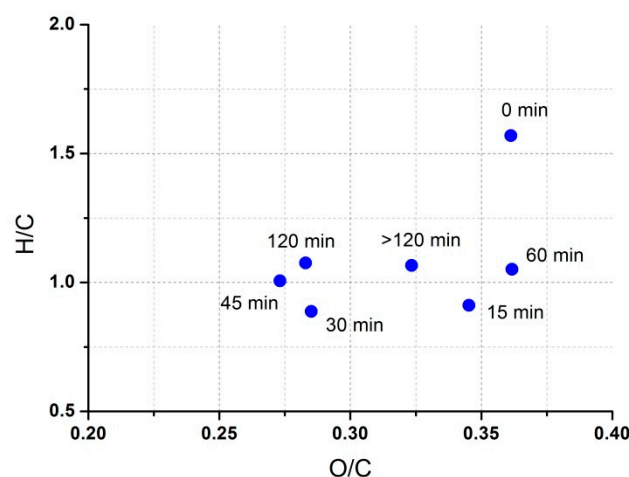
**Table 1.** Characterization of LH samples at different synthesis time.

Sample	pH	% to DM			% to OM		w% Ash Free Basis					Total Acidity, meq g <sup>-1</sup>
		DM, %	Ash	OM	HLF	C	H	N	S	O		
LS	5.21	42.9	22.1	77.9	NA *	55.5	7.3	0.9	9.6	26.7	1.048	
15 min	10.12	26.6	36.3	63.7	30.2	57.9	4.4	0.5	10.5	26.6	0.210	
30 min	9.18	26.4	39.1	60.9	51.9	60.0	4.5	0.7	12.1	22.8	0.293	
45 min	9.01	26.4	39.3	60.7	57.5	60.6	5.1	0.8	11.5	22.0	0.677	
60 min	8.69	25.9	36.9	63.1	62.9	57.2	5.1	0.8	9.3	27.6	0.612	
120 min	8.27	24.8	40.0	60.0	75.0	58.9	5.3	1.1	12.5	22.2	0.643	
>120 min	8.09	21.7	37.7	62.3	71.2	57.3	5.1	0.9	11.9	24.7	0.650	

\* Not applicable.

The C content in the initial LS was 56% and increased to 61% during the first 45 min of oxidation. This fact indicates the formation of more condensed organic compounds. After 60 min, the C content stabilized at a level of 57–58%, which can be interpreted as the formation of stable products of a certain composition. The content of N did not change significantly, being at a level of about 0.5–1%. Sulfur, the essential element in LS, varied within 9–12%.

The dynamics of the OM composition of the samples are clearly traced in the diagram of atomic ratios (Figure 1). The raw material significantly differed from the LH samples in the widest H/C ratio, probably due to the presence of aliphatic moieties. At the initial stage of oxidation, there is a drastic decrease in H/C and a slight decrease in O/C. The latter continues to decrease up to 45 min, but at 60 min, secondary oxygen enrichment is observed, probably due to oxidation. The low O/C ratio in the LH samples is consistent with the low acidity (Table 1). During the first 30 min it drastically dropped from 1 to 0.2–0.3 meq g<sup>-1</sup>, and then after 45 min it slightly raised again, most probably due to oxidative carboxylation during treatment.

**Figure 1.** Atomic ratio diagram for LH sampled at different treatment times.

### 3.2. UV-Vis Absorption and Fluorescence

The absorption properties of untreated LS also differed from that of the processed LH samples (Figure 2a). The initial LS is a yellowish solution with the lowest absorbance, a local maximum peak at 285 nm, and a shoulder at 235 nm, which indicates the presence of phenolic compounds. With the increase in the treatment duration (oxidation time) up to 60 min, the absorption drastically increases, whereas the shoulder at 235 nm vanishes, and the intensity of the peak at 285 nm becomes less pronounced. With further treatment (120 min), a slight decrease is observed again. Most probably, first, a decrease in low-molecular phenolic compounds due to polycondensation and synthesis of the HLS with an

increased degree in aromatic condensation occurs, and then the latter is further oxidized and degraded.

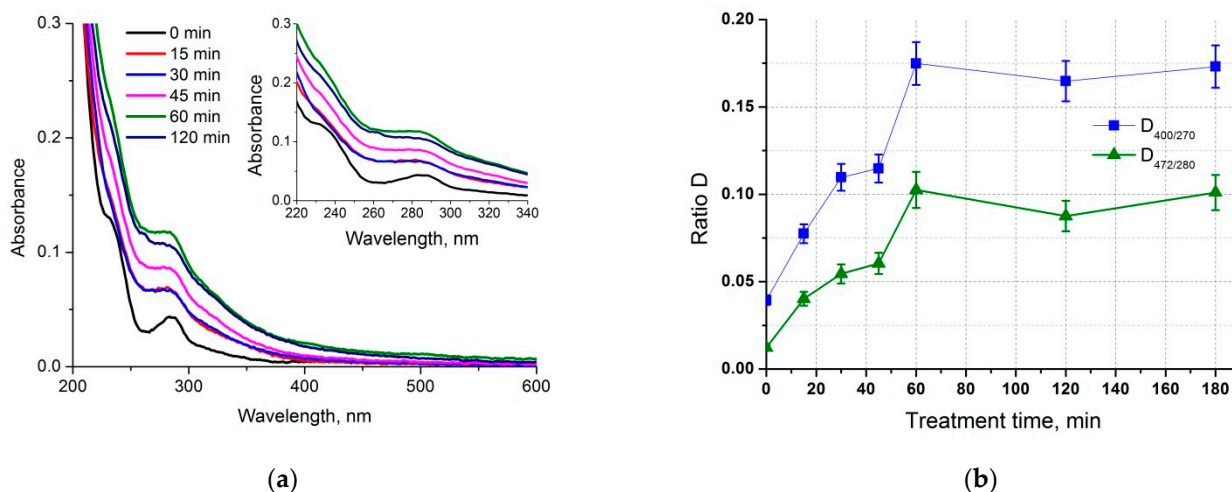


**Figure 2.** UV-absorption spectra, normalized by the OM content (a) and absorbance ratios  $D_{280/472}$  and  $D_{270/400}$  (b) of LH sampled at different treatment time.

To extract more information from the absorption spectra, we calculated the absorbance ratios, which are not dependent on LS concentration and therefore can be used for sample characterization during technological processing with possible concentration alteration. The  $D_{270/400}$  characterizes the proportion of phenolic/quinoid core and simpler carboxylic aromatic compounds [54], and  $D_{280/472}$  reflects the proportion between the lignins and other materials at the beginning of humification [55,56]. To avoid mistakes caused by low absorption values in the visible region, we calculated the reciprocal values  $D_{400/270}$  and  $D_{472/280}$  (Figure 2b). The observed increase in absorbance ratios  $D_{400/270}$  and  $D_{472/280}$  (Figure 2b) demonstrates the presence of more complex chromophores such as charge transfer complexes, quinoid and semi-quinoid arrangements, and aromatic and/or heterocyclic zwitterions (aminochrome), etc. [57], absorbing light at longer wavelengths, in the visible spectral region. Thus, these two indices can indicate changes in the proportions of non-humified and humified material during treatment. Both ratios drastically increased during the first 60 min, then slowly stabilized (Figure 2b). This fact can support the consideration that after 60 min of synthesis, the stable HLS are formed.

Fluorescence spectra of all samples upon excitation at  $\lambda_{ex} = 235, 270,$  and  $310$  showed two overlapping emission bands: with a maximum at  $315$  nm (phenolic fluorescence) and within  $400\text{--}420$  nm (humic-like fluorescence) (Figure 3). The intensity ratio of those bands has been drastically changed during the technological processing; after 15 min of treatment, the UV emission band peaked at  $320$  nm (excited at  $235$  nm) became prevailed in the spectra, and the maximum of the blue band shifted from  $400$  to  $420$  nm. This makes it possible to distinguish the untreated and treated LH samples even at a short duration of the process. This knowledge will help to determine the optimum duration of the process for obtaining a high-quality humic product.

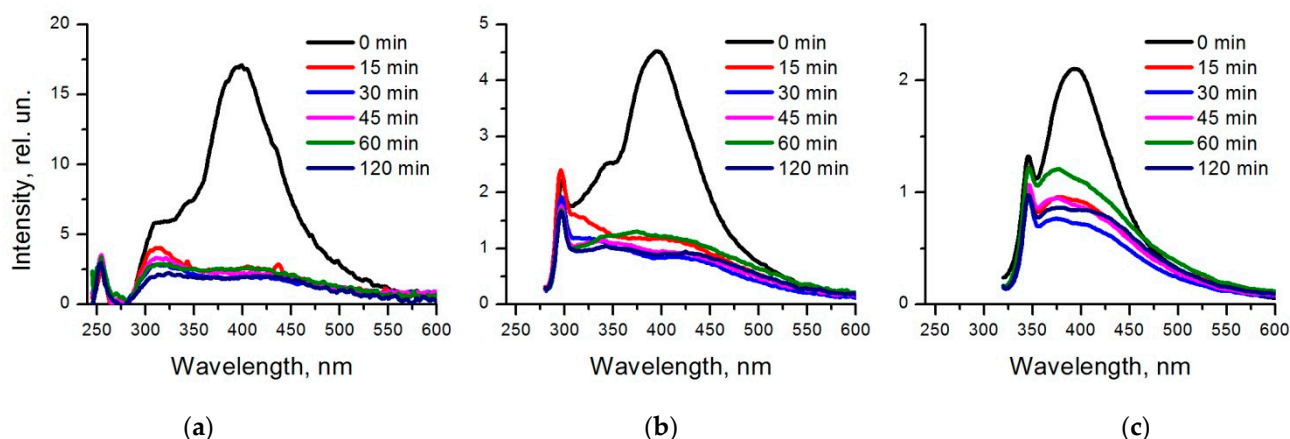


**Figure 3.** Fluorescence emission spectra of initial lignosulfonate (0 min) and LH-samples at different processing periods at excitation wavelengths 235 (a), 270 (b), and 310 nm (c). All spectra were corrected for the “inner-filter” effect.

### 3.3. FTIR-Spectra

The FTIR analysis was performed to evaluate the main chemical attributes of initial LS and LH at different treatment times. The attributions of the main peaks were mainly obtained from references [15,29,58,59].

In the FTIR spectra of all samples studied, there are characteristic absorption bands of the aliphatic C-H bond at  $2940\text{ cm}^{-1}$  and (less pronounced) at  $2840\text{ cm}^{-1}$ . The main absorption bands of functional groups were observed in the region between  $1800$  and  $900\text{ cm}^{-1}$  (Figure 4). A weak band at  $1717\text{ cm}^{-1}$  originated from the C=O stretching vibrations of carboxylic groups was observed only in LS. The pronounced bands at  $1605\text{ cm}^{-1}$  and  $1511\text{ cm}^{-1}$  were assigned to aromatic C=C stretching vibrations.

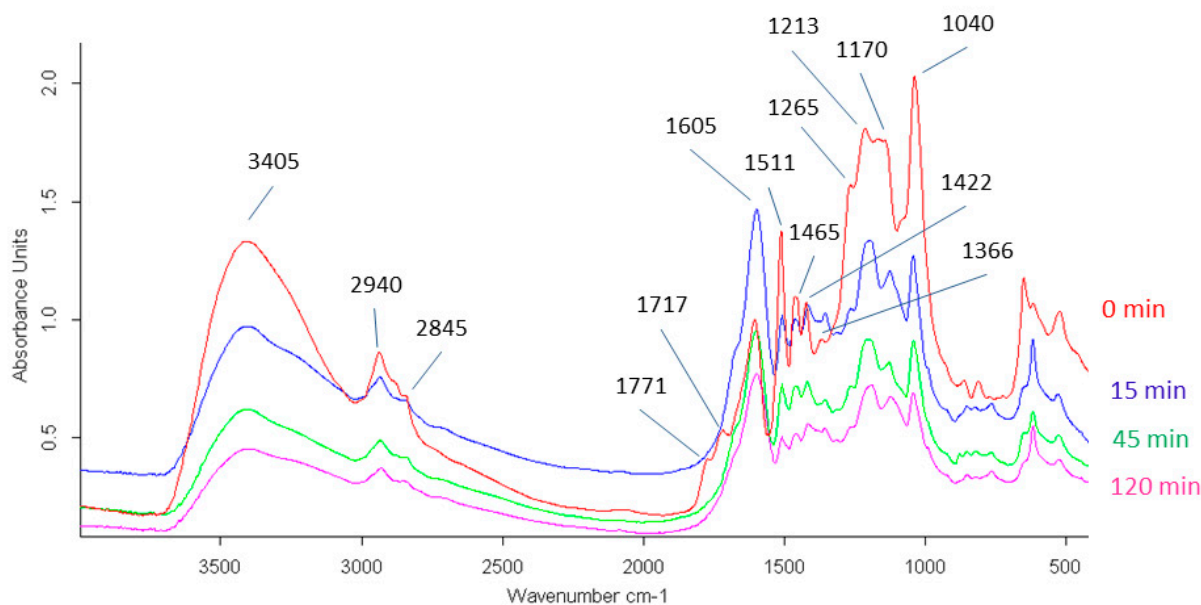


**Figure 4.** FTIR-spectra of LH, sampled at different processing time.

The band at  $1465\text{ cm}^{-1}$  was due to the C-H deformation of aliphatic  $-\text{CH}_3$  and  $-\text{CH}_2$  groups. A band at  $1422\text{ cm}^{-1}$  can be assigned to the C-H deformation in lignin and/or carbohydrates, whereas a band at  $1265\text{ cm}^{-1}$  was due to the guaiacyl ring breathing, C-O stretch in lignin. A band at  $1213\text{ cm}^{-1}$  belonged to the syringyl ring and C-O stretch in lignin, and a double band at  $1143$  and  $1169\text{ cm}^{-1}$  to bending vibrations in the aliphatic

C-OH. The sharp signal at  $1040\text{ cm}^{-1}$  is most probably originated from the  $\text{SO}_3\text{H}$  group vibrations and was observed in all samples.

### 3.4. Bioassay

All the LH samples exhibited certain biological activity on plants (Figure 5). Dry shoots biomass showed insignificant differences ( $p > 0.05$ ), whether root biomass significantly ( $p < 0.01$ ) increased and after 30 min provided a 17–24% increment. The highest growth promotion effect was recorded for the 60 min-sample. Noteworthy that the sample with the highest content of HLF (120 min) showed lower stimulation of seedlings. The probable reason could be the amount and composition of FLF, which contained non-humic compounds (carbohydrates, low molecular weight organic acids), and some of them could be biologically active. Finally, the biological activity of LH could be determined by the emergent properties of the HLS rather than by the quantity and structure of HLF.

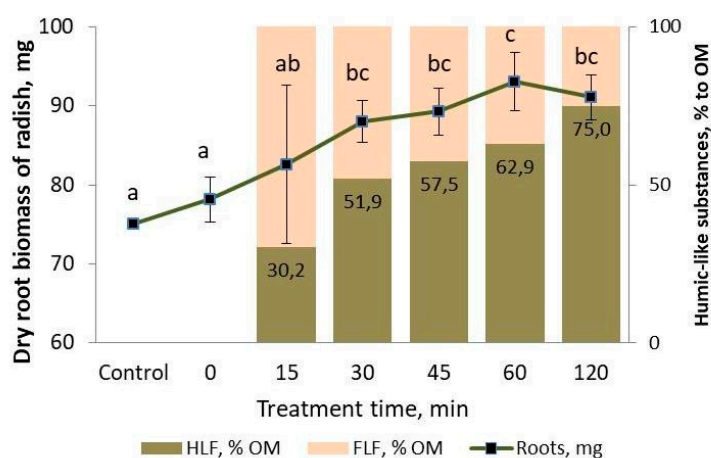


**Figure 5.** Dry root biomass of radish seedlings, treated with LH, sampled at different processing times (mean  $\pm$  SD,  $n = 3$ ). Different letters denote significant differences at the 0.05 confidence level between the treatments according to Fisher's test.

## 4. Discussion

### 4.1. Overview of Results

The obtained data show that during the hydrolytic oxidation, the substantial transformation of LS and synthesis of HLS occur. The initial LS is an acid solution (pH about 5), containing 78% of OM consisting of non-humic lignin-originated substances (Table 1). The C content of 55%, H/C ratio of 1.6, and O/C of 0.4 are typical for lignins [60] (Table 1 and Figure 1). The total acidity of  $1\text{ meq g}^{-1}$  is probably mostly determined by sulfonic acid groups [23], which are also detected by FTIR as an intensive peak at  $1040\text{ cm}^{-1}$  (Figure 4). The shoulder at 235 nm and peak at 285 nm on the absorption spectra (Figure 2a) and the high intensity of fluorescence emission at 315 nm (Figure 3), prove the presence of low-molecular phenolic units [45–48]. In bioassay, LS did not provide any significant promotion of plant growth (Figure 5).

During treatment, all these parameters change. Thus, the content of HLS gradually increases and reaches the maximum (75%) after 2 h of treatment (Table 1). Further treatment does not provide a higher yield in HLS. In contrast, it decreases due to decomposition.

After mixing with alkali, the pH first drastically raises from 5 to 10 during the first 15 min and then gradually goes down to pH 9–8 (Table 1). This fact, along with the dynamics of total acidity (a drop in the first 30 min and an increase from 45 min) (Table 1), indicates the process of oxidative carboxylation, similar to the one that occurs during the humification of lignin in nature [61,62]. As shown on the atomic ratio diagram (Figure 1), H/C ratios decrease from 1.6 to 0.9–1 during 45 min, then slightly go up. This fact also supports the consideration that lignin moieties first transform into more condensed units and then decompose.

Thus, the combination of chemical and spectral data allows concluding that during the thermal hydrolytic-oxidative conversion of LS, processes similar to natural humification occur. Namely, oxidative carboxylation, demetoxilation, and polycondensation. After 45–60 min of processing due to continuous oxidation, the new-formed HLS are subjected to decomposition.

The biological activity of the LH samples of different treatment times generally follows the trend of HLF accumulation (Figure 5). However, the highest plant growth stimulation ability was observed not for the sample with the highest HLF content (at 120 min) but the one at 60 min. This indicates that either the quality (in other words, chemical structure) of HLS drastically changed after 60 min or that the non-humic FLF (containing carbohydrates, low molecular weight organic acids, and minor residual amino acids) also brings a valuable contribution to the manifestation of biological activity. As a biostimulant, LH can promote plant growth due to the complex emergent properties of the whole product rather than by the quantity and structure of HLF.

#### 4.2. Identification of Differences in LH Originated HLS Using Principal Component Analysis

To reveal more accurately the differences in properties and activity of LH as a function of time, we performed principal component analyses (PCA). It enabled us to reveal and generalize the regularities in the changing chemical and spectral properties of the newly formed HLS, depending on synthesis duration.

The PCA yielded two principal components (PC) with eigenvalues of more than one and are responsible for 87% of the total variance of the experimental data (Table 2). PC1 explains 66% of the total variance and shows strong loadings for most of the variables: pH; DM, OM, HLF, H/C, O/C, the intensity of humic and phenolic fluorescence, absorbance at 285 nm, and the root biomass. PC2 explains 23% of the total variances and shows strong loading for acidity and C/N. Thus, the largest contribution (with the loading of more than 0.7) to factor 2 is made by functional groups and the C/N ratio, whereas all other variables contribute to factor 1.

**Table 2.** Factor coordinates of the variables, based on correlations.

Variable	Factor 1	Factor 2
pH	0.812	−0.566
DM, g L <sup>−1</sup>	−0.960	0.038
OM, % DM	−0.990	0.062
HLF, % OM	0.747	0.652
S, %	0.592	0.132
H/C	−0.892	0.445
O/C	−0.781	−0.337
C/N	0.094	−0.988
Total acidity, meq g <sup>−1</sup>	−0.627	0.746
IF phen ( $\lambda_{ex}$ 270)	−0.892	−0.420
IF hum ( $\lambda_{ex}$ 270)	−0.987	0.137
Absorbance D <sub>285</sub>	0.931	0.063
Roots, mg	0.826	0.468
Eigenvalue	8.59	3.03
% Total variance	66.11	23.31
Cumulative %	66.11	89.42

The PCA plot (Figure 6) shows that LH samples can be divided into three groups, depending on the duration of the technological process of HLS synthesis: initial raw material (0-time sample); HLS of 15–30 min, and HLS after 45 min of oxidation. The differences within the samples taken after 45–120 min and more are insignificant. This allows concluding that at these two periods, the samples undergo significant qualitative changes. At the first stage, the decomposition of initial raw material and “artificial humification” resulting

in a synthesis of newly formed HLS occur. At the second stage, the composition of HLS is getting stable, although, to some extent, they are subjected to secondary decomposition.

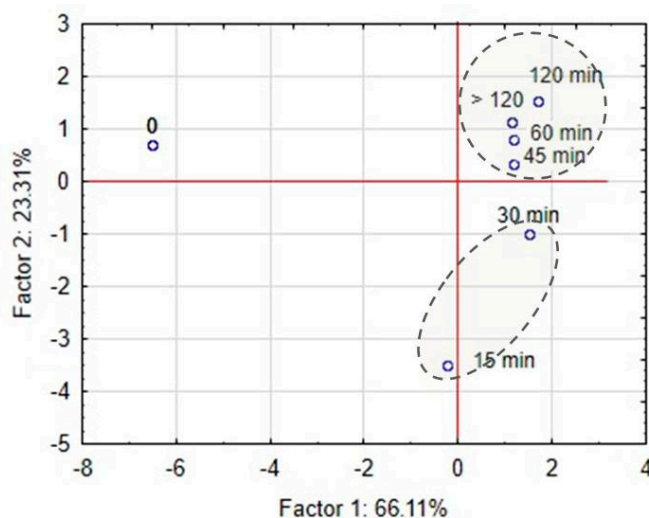


**Figure 6.** Factor score plot for LH sampled at different treatment times.

## 5. Conclusions

Already from the beginning of the oxidation process, a transformation of initial LS and synthesis of HLS occur. During the first 15–30 min, the content of HLF, elemental composition, total acidity, absorption and fluorescence parameters, and the character of FTIR spectra begin to change. The complex of obtained analytical data indicates that at this stage of the technological process, the reactions are similar to those occurring during lignin humification in nature: depolymerization, oxidative carboxylation, and further polycondensation with the formation and accumulation of HLS.

At the second stage, after 45–60 min, the content of HLS reaches a maximum, and its composition stabilizes. However, due to continuous oxidation, the new-formed HLS are subjected to decomposition.

The biological activity, one of the main quality indicators of the final product, reaches a maximum in samples of 45–60 min, before the maximum for HLF (120 min). This indicates that other active compounds, probably low-molecular non-humic substances present in LH, also affect the manifestation of biological activity.

In terms of humic product quality, the obtained set of data shows that the technological process of oxidation/synthesis can be stopped after 60 min. At this stage, LH accumulates the HLS with an aromatic core, carboxylic and phenolic functional groups and showing the highest biological activity. Further processing (up to 2 h and more) does not provide any added value to the product.

**Author Contributions:** Conceptualization and methodology, O.G., O.Y. and S.P.; investigation, A.S., D.K., O.O.; writing—original draft preparation, O.Y., S.P. and O.G.; writing—review and editing, O.Y. and S.P. All authors have read and agreed to the published version of the manuscript.

**Funding:** This research was supported by the Development program of the Interdisciplinary Scientific and Educational School of M.V. Lomonosov Moscow State University «Future Planet and Global Environmental Change». Spectral measurements were funded by the Russian Foundation for Basic Research (RFBR), grant number 19-05-00056.

**Institutional Review Board Statement:** Ethical review and approval were waived for this study, because the study does not involve humans or animals.

**Informed Consent Statement:** Not applicable for studies not involving humans.

**Acknowledgments:** Authors acknowledge the staff of the analytical laboratory and technologists of LTD RET for their assistance in collecting of samples.

**Conflicts of Interest:** The authors declare no conflict of interest.

## References

1. Olk, D.C.; Dinnes, D.L.; Scoresby, J.R.; Callaway, C.R.; Darlington, J.W. Humic products in agriculture: Potential benefits and research challenges—a review. *J. Soils Sediments* **2018**, *18*, 2881–2891. [[CrossRef](#)]
2. Conselvan, G.B.; Pizzeghello, D.; Francioso, O.; Di Foggia, M.; Nardi, S.; Carletti, P. Biostimulant activity of humic substances extracted from leonardites. *Plant Soil* **2017**, *420*, 119–134. [[CrossRef](#)]
3. Pukalchik, M.; Panova, M.; Karpukhin, M.; Yakimenko, O.; Kydralieva, K.; Terekhova, V. Using humic products as amendments to restore Zn and Pb polluted soil: A case study using rapid screening phytotest endpoint. *J. Soils Sediments* **2018**, *18*, 750–761. [[CrossRef](#)]
4. Pukalchik, M.; Kydralieva, K.; Yakimenko, O.; Fedoseeva, E.; Terekhova, V. Outlining the potential role of humic products in modifying biological properties of the soil—a review. *Front. Environ. Sci.* **2019**, *7*, 80. [[CrossRef](#)]
5. Jindo, K.; Olivares, F.L.; da Paixão Malcher, D.J.; Sánchez-Monedero, M.A.; Kempenaar, C.; Canellas, L.P. From lab to field: Role of humic substances under open-field and greenhouse conditions as biostimulant and biocontrol agent. *Front. Plant Sci.* **2020**, *11*, 426. [[CrossRef](#)] [[PubMed](#)]
6. Kulikova, N.A.; Volikov, A.B.; Filippova, O.I.; Kholodov, V.A.; Yaroslavtseva, N.V.; Farkhodov, Y.R.; Yudina, A.V.; Roznyatovsky, V.A.; Grishin, Y.K.; Zhilkibayev, O.T. Modified humic substances as soil conditioners: Laboratory and field trials. *Agronomy* **2021**, *11*, 150. [[CrossRef](#)]
7. Calvo, P.; Nelson, L.; Kloepper, J.W. Agricultural uses of plant biostimulants. *Plant Soil* **2014**, *383*, 3–41. [[CrossRef](#)]
8. Canellas, L.P.; Olivares, F.L.; Aguiar, N.O.; Jones, D.L.; Nebbioso, A.; Mazzei, P.; Piccolo, A. Humic and fulvic acids as biostimulants in horticulture. *Sci. Hortic.* **2015**, *196*, 15–27. [[CrossRef](#)]
9. Ertani, A.; Francioso, O.; Tugnoli, V.; Righi, V.; Nardi, S. Effect of commercial lignosulfonate-humate on *Zea mays* L. metabolism. *J. Agric. Food Chem.* **2011**, *59*, 11940–11948. [[CrossRef](#)]
10. Laurichesse, S.; Averous, L. Chemical modification of lignins: Towards biobased polymers. *Prog. Polym. Sci.* **2014**, *39*, 1266–1290. [[CrossRef](#)]
11. Savy, D.; Canellas, L.; Vinci, G.; Cozzolino, V.; Piccolo, A. Humic-like water-soluble lignins from giant reed (*Arundo donax* L.) display hormone-like activity on plant growth. *J. Plant Growth Regul.* **2017**, *36*, 995–1001. [[CrossRef](#)]
12. Gargulak, J.D.; Lebo, S.E. Commercial use of lignin-based materials. *Lignin Hist. Biol. Mater. Perspect.* **2000**, *742*, 304–320. [[CrossRef](#)]
13. Yakimenko, O.S.; Terekhova, V.A. Humic preparations and the assessment of their biological activity for certification purposes. *Eurasian Soil Sci.* **2011**, *44*, 1222–1230. [[CrossRef](#)]
14. Rose, M.T.; Patti, A.F.; Little, K.R.; Brown, A.L.; Jackson, W.R.; Cavagnaro, T.R. A Meta-analysis and review of plant-growth response to humic substances: Practical implications for agriculture. *Adv. Agron.* **2014**, *124*, 37–89. [[CrossRef](#)]
15. Ertani, A.; Nardi, S.; Francioso, O.; Pizzeghello, D.; Tinti, A.; Schiavon, M. Metabolite-targeted analysis and physiological traits of *Zea mays* L. in response to application of a leonardite-humate and lignosulfonate-based products for their evaluation as potential biostimulants. *Agronomy* **2019**, *9*, 445. [[CrossRef](#)]
16. Popa, V.I. Lignin in Biological Systems. *Polym. Biomater. Struct. Funct.* **2013**, *1*, 709–737. [[CrossRef](#)]
17. Almas, A.R.; Afanou, A.K.; Krogstad, T. Impact of lignosulfonate on solution chemistry and phospholipid fatty acid composition in soils. *Pedosphere* **2014**, *24*, 308–321. [[CrossRef](#)]
18. Savy, D.; Cozzolino, V.; Drosos, M.; Mazzei, P.; Piccolo, A. Replacing calcium with ammonium counterion in lignosulfonates from paper mills affects their molecular properties and bioactivity. *Sci. Total Environ.* **2018**, *645*, 411–418. [[CrossRef](#)] [[PubMed](#)]
19. Abdullah, W.; Tan, N.P.; Low, L.Y.; Loh, J.Y.; Wee, C.Y.; Taib, A.Z.M.; Ong-Abdullah, J.; Lai, K.S. Calcium lignosulfonate improves proliferation of recalcitrant indica rice callus via modulation of auxin biosynthesis and enhancement of nutrient absorption. *Plant Physiol. Biochem.* **2021**, *161*, 141–152. [[CrossRef](#)]
20. Ikkonen, E.; Chazhengina, S.; Jurkevich, M. Photosynthetic nutrient and water use efficiency of *Cucumis sativus* under contrasting soil nutrient and lignosulfonate levels. *Plants* **2021**, *10*, 340. [[CrossRef](#)]
21. Lamar, R.T.; Olk, D.C.; Mayhew, L.; Bloom, P.R. A new standardized method for quantification of humic and fulvic acids in humic ores and commercial products. *J. Aoac Int.* **2014**, *97*, 721–730. [[CrossRef](#)]
22. Karpukhina, E.; Mikheev, I.; Perminova, I.; Volkov, D.; Proskurnin, M. Rapid quantification of humic components in concentrated humate fertilizer solutions by FTIR spectroscopy. *J. Soils Sediments* **2019**, *19*, 2729–2739. [[CrossRef](#)]
23. Matsushita, Y. Conversion of technical lignins to functional materials with retained polymeric properties. *J. Wood Sci.* **2015**, *61*, 230–250. [[CrossRef](#)]
24. Savy, D.; Mazzei, P.; Nebbioso, A.; Drosos, M.; Nuzzo, A.; Cozzolino, V.; Spaccini, R.; Piccolo, A. Molecular properties and functions of humic substances and humic-like substances (HULIS) from biomass and their transformation products. In *Analytical Techniques and Methods for Biomass*; Springer: Berlin, Germany, 2016; pp. 85–114.
25. Wang, W.; Hou, Y.; Huang, W.; Liu, X.; Wen, P.; Wang, Y.; Yu, Z.; Zhou, S. Alkali lignin and sodium lignosulfonate additives promote the formation of humic substances during paper mill sludge composting. *Bioresour. Technol.* **2021**, *320*, 124361. [[CrossRef](#)] [[PubMed](#)]

26. Poloskin, R.B.; Polyakov, Y.U.; Gladkov, O.A.; Sokolova, I.V.; Sorokin, N.I.; Glebov, A.V.; Polyakov, Y.J.; Sorokin, N. Humic acid salts preparation involves high-temperature treatment of an aqueous suspension of raw vegetable material in a continuous process. U.S. Patent 7198805-B2, 3 April 2021.
27. Katahira, R.; Mittal, A.; McKinney, K.; Chen, X.W.; Tucker, M.P.; Johnson, D.K.; Beckham, G.T. Base-catalyzed depolymerization of biorefinery lignins. *ACS Sustain. Chem. Eng.* **2016**, *4*, 1474–1486. [[CrossRef](#)]
28. Lyu, G.J.; Yoo, C.G.; Pan, X.J. Alkaline oxidative cracking for effective depolymerization of biorefining lignin to mono-aromatic compounds and organic acids with molecular oxygen. *Biomass Bioenergy* **2018**, *108*, 7–14. [[CrossRef](#)]
29. Novak, F.; Sestauberova, M.; Hrabal, R. Structural features of lignohumic acids. *J. Mol. Struct.* **2015**, *1093*, 179–185. [[CrossRef](#)]
30. Abdelaziz, O.Y.; Meier, S.; Prothmann, J.; Turner, C.; Riisager, A.; Hulteberg, C.P. Oxidative depolymerisation of lignosulphonate lignin into low-molecular-weight products with Cu-Mn/ $\delta$ -Al<sub>2</sub>O<sub>3</sub>. *Top. Catal.* **2019**, *62*, 639–648. [[CrossRef](#)]
31. Pinto, P.C.R.; da Silva, E.A.B.; Rodrigues, A.E. Insights into oxidative conversion of lignin to high-added-value phenolic aldehydes. *Ind. Eng. Chem. Res.* **2011**, *50*, 741–748. [[CrossRef](#)]
32. Santos, S.G.; Marques, A.P.; Lima, D.L.D.; Evtuguin, D.V.; Esteves, V.I. Kinetics of eucalypt lignosulfonate oxidation to aromatic aldehydes by oxygen in alkaline medium. *Ind. Eng. Chem. Res.* **2011**, *50*, 291–298. [[CrossRef](#)]
33. Cui, P.; Fang, H.X.; Qian, C.; Cheng, M.H. Detection and identification of lignosulfonate depolymerization products using UPLC-QTOF-MS and a self-built database. *Chromatographia* **2020**, *83*, 87–93. [[CrossRef](#)]
34. Pu, Y.Q.; Hu, F.; Huang, F.; Ragauskas, A.J. Lignin structural alterations in thermochemical pretreatments with limited delignification. *Bioenergy Res.* **2015**, *8*, 992–1003. [[CrossRef](#)]
35. El Mansouri, N.E.; Farriol, X.; Salvado, J. Structural modification and characterization of lignosulfonate by a reaction in an alkaline medium for its incorporation into phenolic resins. *J. Appl. Polym. Sci.* **2006**, *102*, 3286–3292. [[CrossRef](#)]
36. Guizani, C.; Lachenal, D. Controlling the molecular weight of lignosulfonates by an alkaline oxidative treatment at moderate temperatures and atmospheric pressure: A size-exclusion and reverse-phase chromatography study. *Int. J. Mol. Sci.* **2017**, *18*, 2520. [[CrossRef](#)]
37. Schutyser, W.; Kruger, J.S.; Robinson, A.M.; Katahira, R.; Brandner, D.G.; Cleveland, N.S.; Mittal, A.; Peterson, D.J.; Meilan, R.; Roman-Leshkov, Y.; et al. Revisiting alkaline aerobic lignin oxidation. *Green Chem.* **2018**, *20*, 3828–3844. [[CrossRef](#)]
38. Hladky, J.; Pospisilova, L.; Liptaj, T. Spectroscopic characterization of natural humic substances. *J. Appl. Spectrosc.* **2013**, *80*, 8–14. [[CrossRef](#)]
39. Enev, V.; Pospisilova, L.; Klucakova, M.; Liptaj, T.; Duskocil, L. Spectral Characterization of Selected Humic Substances. *Soil Water Res.* **2014**, *9*, 9–17. [[CrossRef](#)]
40. Jarosova, M.; Klejdus, B.; Kovacik, J.; Hedbavny, J. The impact of humic substances on oxidative stress and plant growth of spring barley exposed to NaCl. *Mendelnet* **2014**, *2014*, 463–468.
41. Yakimenko, O.; Khundzhua, D.; Izosimov, A.; Yuzhakov, V.; Patsaeva, S. Source indicator of commercial humic products: UV-Vis and fluorescence proxies. *J. Soils Sediments* **2018**, *18*, 1279–1291. [[CrossRef](#)]
42. Poloskin, R.; Gladkov, O.; Osipova, O.; Yakimenko, O. Comparable Evaluation of Biological Activity of New Liquid and Dry Modifications of the Humic Product “Lignohumate”. In *Functions of Natural Organic Matter in Changing Environment*; Springer: Berlin, Germany, 2013; pp. 1095–1099.
43. Suada, I.K.; Suwastika, A.A.N.G.; Pradnyana, I.K.N.; Shchegolkova, N.; Poloskin, R.; Gladkov, O.; Yakimenko, O.; Stepanov, A. Application of *Trichoderma* spp. and Lignohumate to Suppress a Pathogen of Clubroot (*Plasmodiophora Brassicae* Wor.) and Promote Plant Growth of Cabbage. *Int. J. Biosci. Biotechnol.* **2019**, *6*, 79–94. [[CrossRef](#)]
44. Pozdnyakov, L.A.; Stepanov, A.L.; Gasanov, M.E.; Semenov, M.V.; Yakimenko, O.S.; Suada, I.K.; Rai, I.N.; Shchegolkova, N.M. Effect of Lignohumate on Soil Biological Activity on the Bali Island, Indonesia. *Eurasian Soil Sci.* **2020**, *53*, 653–660. [[CrossRef](#)]
45. Garcia, A.C.; de Castro, T.A.V.; Santos, L.A.; Tavares, O.C.H.; Castro, R.N.; Berbara, R.L.L.; Garcia-Mina, J.M. Structure-Property-Function Relationship of Humic Substances in Modulating the Root Growth of Plants: A Review. *J. Environ. Qual.* **2019**, *48*, 1622–1632. [[CrossRef](#)]
46. Perminova, I.V.; Garcia-Mina, J.M.; Knicker, H.; Miano, T. Humic substances and nature-like technologies: Learning from nature: Understanding humic substances structures and interactions for the development of environmentally friendly, nature-like technologies. *J. Soils Sediments* **2019**, *19*, 2663–2664. [[CrossRef](#)]
47. Savy, D.; Brostaux, Y.; Cozzolino, V.; Delaplace, P.; du Jardin, P.; Piccolo, A. Quantitative Structure-Activity Relationship of Humic-Like Biostimulants Derived From Agro-Industrial Byproducts and Energy Crops. *Front. Plant Sci.* **2020**, *11*, 581. [[CrossRef](#)] [[PubMed](#)]
48. Du Jardin, P. Plant biostimulants: Definition, concept, main categories and regulation. *Sci. Hortic.* **2015**, *196*, 3–14. [[CrossRef](#)]
49. De Pascale, S.; Roupheal, Y.; Colla, G. Plant biostimulants: Innovative tool for enhancing plant nutrition in organic farming. *Eur. J. Hortic. Sci* **2017**, *82*, 277–285. [[CrossRef](#)]
50. Yakhin, O.I.; Lubyantsev, A.A.; Yakhin, I.A.; Brown, P.H. Biostimulants in Plant Science: A Global Perspective. *Front. Plant Sci.* **2017**, *7*, 2049. [[CrossRef](#)]
51. Swift, R.S. Organic matter characterization. *Methods Soil Anal.* **1996**, *5*, 1011–1069.
52. Gosteva, O.Y.; Izosimov, A.A.; Patsaeva, S.V.; Yuzhakov, V.I.; Yakimenko, O.S. Fluorescence of Aqueous Solutions of Commercial Humic Products. *J. Appl. Spectrosc.* **2012**, *78*, 884–891. [[CrossRef](#)]

53. Khundzhua, D.A.; Patsaeva, S.V.; Trubetskoj, O.A.; Trubetskaya, O.E. An Analysis of Dissolved Organic Matter from Freshwater Karelian Lakes Using Reversed-Phase High-Performance Liquid Chromatography with Online Absorbance and Fluorescence Analysis. *Mosc. Univ. Phys. Bull.* **2017**, *72*, 68–75. [[CrossRef](#)]
54. Uyguner, C.S.; Bekbolet, M. Evaluation of humic acid photocatalytic degradation by UV-vis and fluorescence spectroscopy. *Catal. Today* **2005**, *101*, 267–274. [[CrossRef](#)]
55. Domeizel, M.; Khalil, A.; Prudent, P. UV spectroscopy: A tool for monitoring humification and for proposing an index of the maturity of compost. *Bioresour. Technol.* **2004**, *94*, 177–184. [[CrossRef](#)]
56. Albrecht, R.; Le Petit, J.; Terrom, G.; Perissol, C. Comparison between UV spectroscopy and NIRS to assess humification process during sewage sludge and green wastes co-composting. *Bioresour. Technol.* **2011**, *102*, 4495–4500. [[CrossRef](#)] [[PubMed](#)]
57. Lipski, M.; Slawinski, J.; Zych, D. Changes in the luminescent properties of humic acids induced by UV radiation. *J. Fluoresc.* **1999**, *9*, 133–138. [[CrossRef](#)]
58. Senesi, N.; D’Orazio, V.; Ricca, G. Humic acids in the first generation of EUROSOILS. *Geoderma* **2003**, *116*, 325–344. [[CrossRef](#)]
59. Fuentes, M.; Baigorri, R.; Gonzalez-Gaitano, G.; Garcia-Mina, J.M. New methodology to assess the quantity and quality of humic substances in organic materials and commercial products for agriculture. *J. Soils Sediments* **2018**, *18*, 1389–1399. [[CrossRef](#)]
60. Zherebker, A.; Kostyukevich, Y.; Kononikhin, A.; Kharybin, O.; Konstantinov, A.I.; Zaitsev, K.V.; Nikolaev, E.; Perminova, I.V. Enumeration of carboxyl groups carried on individual components of humic systems using deuteromethylation and Fourier transform mass spectrometry. *Anal. Bioanal. Chem.* **2017**, *409*, 2477–2488. [[CrossRef](#)]
61. Stevenson, F.J. *Humus Chemistry: Genesis, Composition, Reactions*; John Wiley & Sons: Hoboken, NJ, USA, 1994.
62. Tan, K.H. *Humic Matter in Soil and the Environment: Principles and Controversies*, 2nd ed.; CRC Press: Boca Raton, FL, USA, 2014; pp. 1–439. [[CrossRef](#)]